Electronic Supplementary Material

Superfluorinated and NIR-luminescent Gold Nanoclusters

V. Dichiarante,†[a,b] I. Tirotta,†[a,b,c] L. Catalano,[b] G. Terraneo,[a,b] G. Raffaini,[b] M. R. Chierotti,[d] R. Gobetto,[d] F. Baldelli Bombelli*[a,b] and P. Metrangolo*[a,b,c,e]

[a] *Fondazione Centro Europeo Nanomedicina, Politecnico di Milano, Milan, Italy*

[b] *Department of Chemistry, Materials and Chemical Engineering "Giulio Natta", Politecnico di Milano, Milan, Italy*

[c] *Center for Nano Science&Technology IIT@POLIMI (CNST), Milan, Italy.*

[d] *Department of Chemistry and NIS, University of Turin, Italy*

[e] *VTT Technical Research Center of Finland Ltd, Biologinkuja 7, 02150 Espoo, Finland*

Corresponding authors (*):

Francesca Baldelli Bombelli, Department of Chemistry, Materials and Chemical Engineering ''Giulio Natta'', Politecnico di Milano, via L. Mancinelli 7, IT-20131 Milan, Italy. Phone: +39 02 2399 4745, Fax: +39 02 2399 3180, E-mail: francesca.baldelli@polimi.it

Pierangelo Metrangolo, Department of Chemistry, Materials and Chemical Engineering ''Giulio Natta'', Politecnico di Milano, via L. Mancinelli 7, IT-20131 Milan, Italy. Phone: +39 02 2399 3041, Fax: +39 02 2399 3180, E-mail: pierangelo.metrangolo@polimi.it

Table of Contents

General information

1. Materials and methods

Starting materials were purchased from Sigma-Aldrich, Fluorochem, Apollo Scientific and used as received. Commercial HPLC-grade solvents were used without further purification. Anhydrous tetrahydrofuran (THF) was obtained by distillation over sodium/benzophenone before use, whereas anhydrous dichloromethane (DCM) was purchased from Sigma-Aldrich. Solkane® (1,1,1,3,3-pentafluorobutane) was purchased from Solvay and filtered through a 0.2 μm PTFE membrane before use. Milli-Q water was obtained by a Simplicity (Millipore) instrument.

Analytical thin layer chromatography (TLC) was performed on precoated silica gel 60 F254 plates and visualization was done by staining with 0.2 M aqueous $KMnO_4$.

DSC analyses were performed on a Mettler Toledo DSC823e differential scanning calorimeter, using aluminium 40 μL sample pans and Mettler STARe software for calculation. Melting points were also determined on a Reichert instrument, by observing the melting process through an Olympus BH-2 optical microscope.

2. Mass spectrometry

Low resolution Electrospray Ionization (ESI) mass spectra were recorded on a ESI Ion Trap LC/MSn System (BRUKER Esquire 3000 PLUS).

Accurate mass analyses were carried out by a VG Autospec M246 (Fisons) having a E1BE2 geometry.

For ICP mass determination of gold content, 100 μL of each sample were added to 4 mL of a concentrated HNO_3 / HCl (1:3) mixture in a Teflon digestion vessel. The samples were digested in a Milestone Ethos TC microwave mineralizer, by heating to 220 °C over 10 minutes and keeping that temperature for 15 minutes. The samples were then diluted to 10 mL with Milli-Q water. ICP-MS analyses were performed on an Inductively Coupled Plasma - Optical Emission Spectroscopy (ICP-OES) Optima 7000 DV (PerkinElmer), with WinLab32 control software. Analyses were performed at 242.795 and 267.595 nm and results are given in ppm (mg/L), as an average of three measurements.

An Autoflex II instrument from Bruker Daltoniks (Bremen, Germany) equipped with a UV/N2-laser (337

nm/100 lJ) was used to carry out MALDI analyses. Saturated trans-2-[3-(4-tertbutylphenyl)-2-methyl-2-propenylidene]malononitrile (DCTB) in solkane was used as the matrix. The purified fluorinated nanoclusters and DCTB, both dissolved in solkane, were mixed in a 1:1 (v/v) ratio and applied on the stainless steel target plate in 1 μL aliquots. The sample spot was dried in air at room temperature. The mass spectrum (4-20 kDa) was measured in linear positive-ion mode, tipically performing 1500 scans, and Protein standard solution II (Bruker Daltonics) was used for the external molecular mass calibration.

3. Transmission Electron Microscopy

TEM images were acquired by using a Philips CM200 TEM, equipped with a field emission gun and operating at 200 kV. Samples were prepared by dropping nanoclusters diluted solutions on carbon-coated copper grids and leaving them drying overnight. TEM image analysis was performed using ImageJ software. Statistical analysis was based on the measurement of about 1000-4000 NPs. Size distributions were fitted by a Gaussian equation using IgorPro 4.02.

4. Infrared spectroscopy

Attenuated total reflectance FTIR (ATR-FTIR) spectra were obtained with a Thermo Scientific Nicolet iS50 FTIR spectrometer, equipped with an iS50 ATR accessory (Thermo Scientific, Madison, USA). The values were given in wavenumbers and were rounded to 1 cm^{-1} upon automatic assignment. Nanoclusters stock solutions were deposited by drop casting on the ATR probe and the solvent was let to evaporate before starting the measurement.

5. Nuclear Magnetic Resonance

^{1}H, ^{13}C NMR spectra were recorded at room temperature on a Bruker AV400 or AV500 spectrometer. ^{1}H and ^{13}C chemical shifts were referenced to tetramethylsilane (TMS) using the residual proton or carbon impurities of the deuterated solvents as standard reference. Chemical shifts are reported in parts per million (ppm). Multiplicities are reported as follows: s (singlet), brs (broad singlet), d (doublet), t (triplet), q (quartet), dd (doublet of doublets), qui (quintet), m (multiplet).

NMR spectra of fluorinated gold nanoclusters were recorded directly on stock solutions, using a capillary filled with deuterated benzene (C_6D_6) for the locking.

^{19}F NMR spectra as well as ^{19}F T_1 and T_2 measurements were recorded at 293 K on a Jeol ECZR 600 spectrometer operating at 564.73 MHz for the ^{19}F nucleus. ^{19}F chemical shifts were referenced to an internal $CFCl_3$ standard. For quantitative spectra, relaxation delays equal to 5 times the T_1 were used for 256 scans. The inversion recovery and the cpmg pulse sequences were used for the measure of T_1 and T_2, respectively.

6. Optical characterization

UV-vis spectra of fluorinated gold nanoclusters dissolved in Solkane at the appropriate dilution were acquired at room temperature on a V-630 double beam Jasco spectrophotometer, equipped with a halogen lamp and a deuterium lamp.

Fluorescence measurements of fluorinated gold nanoclusters were performed at room temperature using a Nanolog Horiba JobinYvon, equipped with a 450W Xenon short-arc excitation source. Quantum yields were measured with a dual detector made of InGaAs (800 – 160 nm) on Si (400 – 1100 nm), whose baseline signals were corrected and aligned in the range 400 – 1475 nm, using a standard calibrated W lamp (ocean Optics). Measurements were repeated on three different dilutions of the starting NCs stock solution.

7. DLS Multiangle analysis

Dynamic Light Scattering measurements were performed on an ALV apparatus equipped with ALV-5000/EPP Correlator, special optical fiber detector and ALV/CGS-3 Compact goniometer. The light source is He-Ne laser (λ = 633 nm), 22 mW output power. Measurements were performed at 25 °C. Approximately 1 mL of sample solution was transferred into the cylindrical Hellma scattering cell. Data analysis has been performed according to standard procedures and auto-correlation functions were analyzed through a constrained regularization method (Laplace inversion of the time auto-correlation functions), CONTIN, for obtaining the particle size distribution.

Synthesis of thiol 1

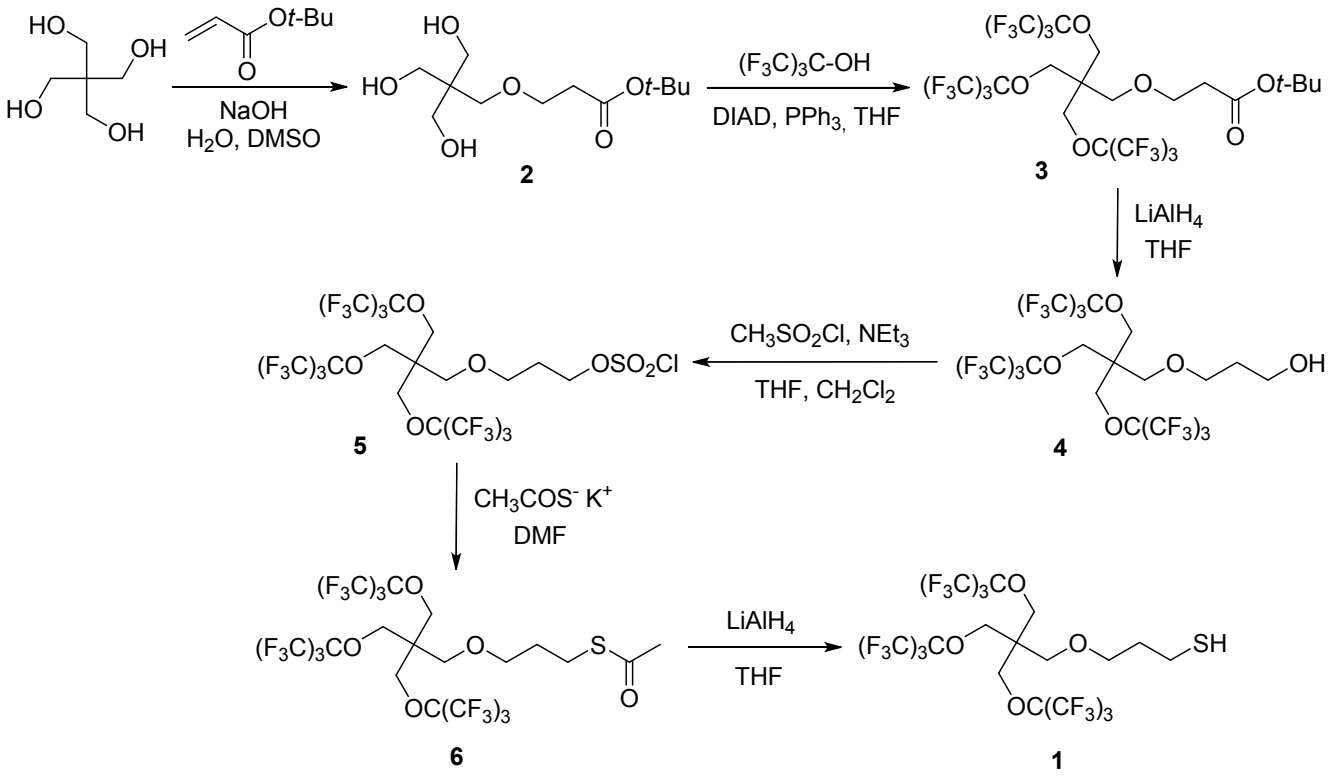

Thiol **1** was synthesized following the procedure reported by Yue *et al.*,[S1] with slight modifications as detailed below.

***tert*-Butyl 3-(3-hydroxy-2,2-bis(hydroxymethyl)propoxy)-propanoate (2)**

Following the same procedure described by Yue,[S1] compound **2** was obtained in 38% yield as a colorless oil, eluting with CH_2Cl_2/CH_3OH (from 98:2 to 9:1).

^{1}H NMR (500 MHz, $CDCl_3$) δ: 3.69 (t, 2H, J = 5.8 Hz), 3.67 (s, 6H), 3.56 (s, 2H), 2.48 (t, 2H, J = 5.8 Hz), 2.35 (brs, 3H), 1.46 (s, 9H).

***tert*-Butyl 3-(3-((1,1,1,3,3,3-hexafluoro-2-(trifluoromethyl)-propan-2-yl)oxy)-2,2-bis(((1,1,1,3,3,3-hexa-fluoro-2-(trifluoromethyl)propan-2-yl)oxy)methyl)propoxy)propanoate (3)**

Triphenylphosphine (30 g, 115 mmol) and 4 Å molecular sieves (3.5 g) were placed in an oven-dried 500 mL flask, under nitrogen flow. Compound **2** (6 g, 23 mmol) and anhydrous THF (150 mL) were added and the solution was cooled to 0 °C. Diisopropylazodicarboxylate (DIAD, 22 mL, 115 mmol) was

added dropwise under stirring. The resulting foamy mixture was warmed up to r.t. and stirred for additional 20 minutes, before adding perfluoro-*tert*-butyl alcohol (16 mL, 115 mmol) in one portion. The finally clear solution was stirred at 45 °C for 65 hours. After cooling down to r.t. and removing the molecular sieves by filtration, water (100 mL) was added and stirring was continued for 10 more minutes. Dichloromethane (50 mL) was added and the lower organic phase was separated, dried over Na_2SO_4 and concentrated under vacuum. Flash silica gel chromatography of the crude with hexane/ethyl acetate (98:2) gave product **3** as a colorless solid (9.5 g, 45% yield).

m.p. 76-78 °C. **^{1}H NMR** (500 MHz, $CDCl_3$) δ: 4.06 (s, 6H), 3.64 (t, 2H, J = 6.5 Hz), 3.43 (s, 2H), 2.45 (t, 2H, J = 6.5 Hz), 1.44 (s, 9H). **^{19}F NMR** (475 MHz, $CDCl_3$) δ: -71.41 (s).

3-(3-((1,1,1,3,3,3-Hexafluoro-2-(trifluoromethyl)propan-2-yl)oxy)-2,2-bis(((1,1,1,3,3,3-hexafluoro-2-(trifluoromethyl)-propan-2-yl)oxy)methyl)propoxy)propan-1-ol (4)

Compound **3** (3 g, 3.3 mmol) was treated with $LiAlH_4$ (360 mg, 9.5 mmol) in anhydrous THF (45 mL) according to the reported procedure.[S1] Purification of the crude by SiO_2 chromatography with hexane/ethyl acetate (8:2) afforded alcohol **4** as a colorless oil (2.3 g, 83% yield).

^{1}H NMR (500 MHz, $CDCl_3$) δ: 4.05 (s, 6H), 3.72 (t, 2H, J = 6.2 Hz), 3.54 (t, 2H, J = 6.2 Hz), 3.40 (s, 2H), 1.82 (qui, 2H, J = 6.2 Hz). **^{19}F NMR** (475 MHz, $CDCl_3$) δ: -71.41 (s).

3-(3-((1,1,1,3,3,3-Hexafluoro-2-(trifluoromethyl)propan-2-yl)oxy)-2,2-bis(((1,1,1,3,3,3-hexafluoro-2-(trifluoromethyl)-propan-2-yl)oxy)methyl)propoxy)propyl methanesulfonate (5)

Reaction of **4** (3 g, 3.5 mmol) with triethylamine (1.4 mL, 10 mmol) and methanesulfonyl chloride (0.8 mL, 10 mmol) in a mixture of anhydrous THF (15 mL) and anhydrous DCM (30 mL) was performed as described by Yue.[S1] Flash chromatography over silica gel with hexane/ethyl acetate (8:2) as eluent yielded **5** as a colorless oil (3.1 g, 97% yield).

^{1}H NMR (500 MHz, $CDCl_3$) δ: 4.27 (t, 2H, J = 6.3 Hz), 4.06 (s, 6H), 3.53 (t, 2H, J = 6.1 Hz), 3.42 (s, 2H), 2.98 (s, 3H), 2.00 (qui, 2H, J = 6.3 Hz). **^{19}F NMR** (475 MHz, $CDCl_3$) δ: -71.45 (s).

(*S*)-(3-(3-((1,1,1,3,3,3-Hexafluoro-2-(trifluoromethyl)propan-2-yl)oxy)-2,2-bis(((1,1,1,3,3,3-hexafluoro-2-(trifluoromethyl)-propan-2-yl)oxy)methyl)propoxy)propyl)ethanethioate (6)

A solution of **5** (2.8 g, 3 mmol) in DMF (28 mL) was treated with potassium thioacetate (1.1 g, 9 mmol) at 50 °C, as reported.[S1] Silica gel chromatography, eluting with hexane/ethyl acetate (95:5), gave product **6** as a pale yellow oil (2.3 g, 85% yield).

^{1}H NMR (500 MHz, $CDCl_3$) δ: 4.06 (s, 6H), 3.43 (t, 2H, *J* = 6.1 Hz), 3.38 (s, 2H), 2.89 (t, 2H, *J* = 7.1 Hz), 2.32 (s, 3H), 1.83 (qui, 2H, *J* = 6.6 Hz). **^{19}F NMR** (475 MHz, $CDCl_3$) δ: -71.48 (s).

3-(3-((1,1,1,3,3,3-Hexafluoro-2-(trifluoromethyl)propan-2-yl)oxy)-2,2-bis(((1,1,1,3,3,3-hexafluoro-2-(trifluoromethyl)-propan-2-yl)oxy)methyl)propoxy)propane-1-thiol (1)

Compound **6** (2 g, 2.2 mmol) was treated with $LiAlH_4$ (230 mg, 6 mmol) in anhydrous THF (25 mL), according to Yue's procedure.[S1] Flash chromatography with hexane/ethyl acetate (98:2) afforded thiol **1** as a colorless solid (1.5 g, 81% yield).

m.p. 39-40 °C. **^{1}H NMR** (400 MHz, $CDCl_3$) δ: 4.06 (s, 6H), 3.50 (t, 2H, *J* = 6.1 Hz), 3.40 (s, 2H), 2.56 (dd, 2H, *J* = 7.2 and 15 Hz), 1.89-1.82 (m, 2H), 1.32 (t, 1H, *J* = 7.9 Hz). **^{13}C NMR** (100 MHz, $CDCl_3$) δ: 120.2 (q, *J* = 293 Hz), 79.7 (m), 69.7, 66.2, 65.7, 46.2, 33.6, 21.2. **^{19}F NMR** (475 MHz, $CDCl_3$) δ: -71.57 (s). **FTIR** (cm^{-1}): 1490, 1468, 1243, 1189, 1153, 1122, 1011, 969, 913, 771, 736, 725, 538, 515, 478. **MS (ESI+)** *m/z*: 887 [M+Na]. **HRMS for $C_{20}H_{15}F_{27}O_4S$**: calcd. 864.025994; found 864.023560.

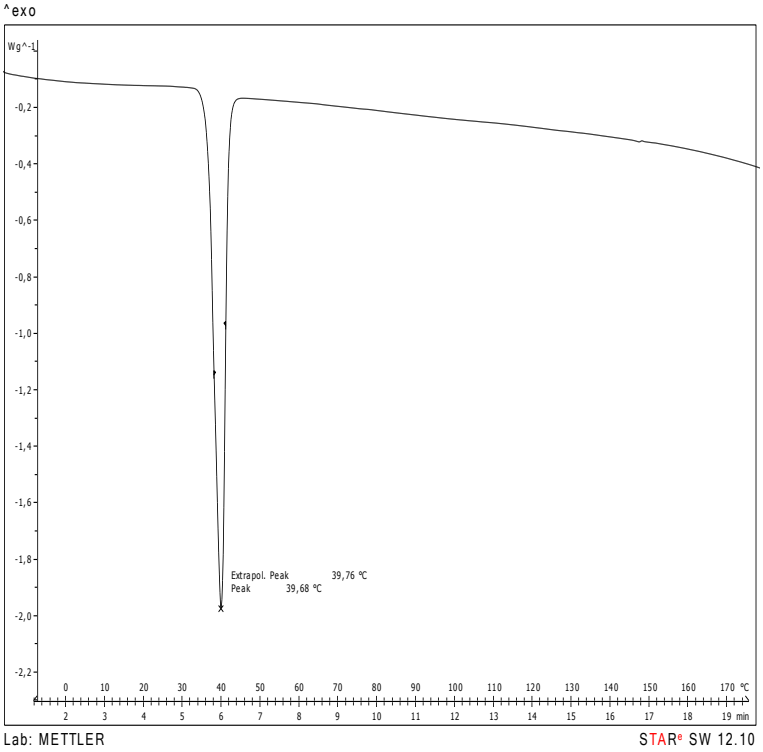

Figure S1. DSC analysis of compound **1** (first heating cycle at 10 °C min^{-1}).

X-ray single crystal analysis

The single crystal X-Ray structure of thiol **1** was determined on a Bruker Kappa Apex II diffractometer at 140 K using a fine-focus sealed MoKα tube, λ=0.71073 Å. Data collection and reduction were performed by SMART and SAINT and absorption correction, based on multi-scan procedure, by SADABS. The structure were solved by SHELXS-97[S2] and refined on all independent reflections by full-matrix least-squares based on F^2 by using SHELXL-97.[S2] All the non-hydrogen atoms were refined anisotropically. Hydrogen atoms were placed in calculated positions and refined by using a riding model. Crystallographic data and structural refinement details are summarized in Table S1. Crystallographic data for the structural analysis have been deposited with the Cambridge Crystallographic Data Center. Figures are obtained with Mercury 3.5[S3] and Chimera.[S4]

Table S1. Crystallographic details of thiol **1**.

Chemical formula	$C_{20}H_{15}F_{27}O_4S$
M_r	864.38
Crystal system, space group	Monoclinic, $P2_1/n$
Temperature (K)	140
a, b, c (Å)	6.7936 (7), 24.851 (3), 17.591 (2)
β (°)	90.105 (4)
V (Å^3)	2969.8 (6)
Z	4
Radiation type	Mo $K\alpha$
μ (mm^{-1})	0.31
Crystal size (mm)	0.18 × 0.16 × 0.12
T_{min}, T_{max}	0.689, 0.746
No. of measured, independent and observed [$I > 2\sigma(I)$] reflections	54783, 6496, 5459
R_{int}	0.032
$(\sin \theta/\lambda)_{max}$ (Å^{-1})	0.642
$R[F^2 > 2\sigma(F^2)]$, $wR(F^2)$, S	0.040, 0.105, 1.01
No. of reflections	6496
No. of parameters	477
H-atom treatment	H atoms treated by a mixture of independent and constrained refinement

$\Delta\rho_{max}$, $\Delta\rho_{min}$ (e Å^{-3})	0.55, -0.27
CCDC number	1479121

X-ray single crystal experimental details

Data were collected at 140 K since all the tested crystals showed a phase transition with loss of crystallinity below that temperature. They showed a very short life-time and sublimated quite fast (due to the high number of fluorine atoms). In general, diffraction appeared very poor and crystals were twinned. Thanks to the referee's suggestions we recognize a possible pseudo-merohedral twinning by a 180 deg rotation around x or z axis. The system was refined as a 2-compontent twin using the card TWIN -1 0 0 0 -1 0 0 0 1. The refinement easily converged at BASF 0.3824 with R1 of 4.4%. Around the atom S1 a strong peak of residual electron density, about 1 e/Ang^3, was detected. We assumed a minor disorder of the sulfur atom, which was split and refined it as an alternative position with 7% occupancy. The H atom at sulfur was found (from difference Fourier map) and refined in isotropic approximation, without restraints.

Even if the quality of the single crystal structure was not high, the structure was used as starting geometry for computational studies and to calculate the molecular volume (515 Å^3), which was used to estimate the number of molecules bound to the nanoparticle surface.

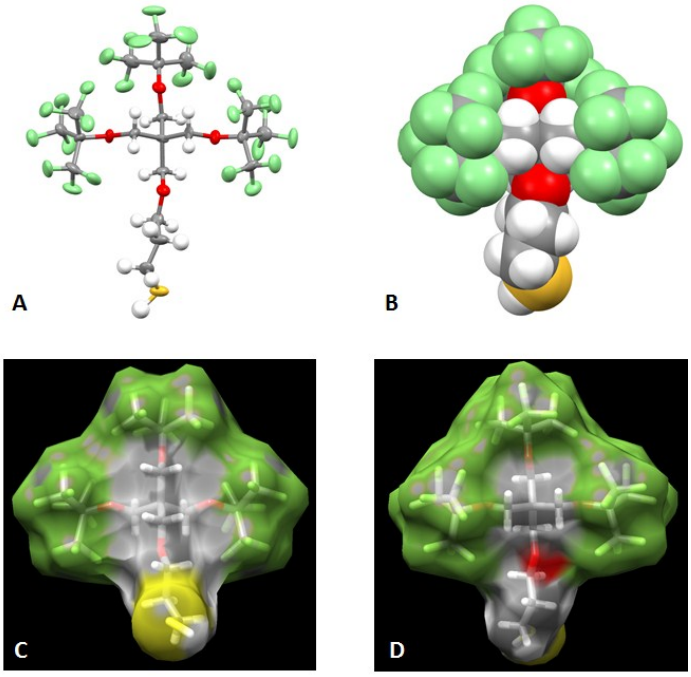

Figure S2. Different representations of single crystal structure of thiol **1**: (A) Ellipsoid representation (50% probability level); (B) Spacefill representation; (C) and (D) Molecular surface of **1**. [Color code: C, gray; H, white; O, red; S, yellow and F, light green]

Synthesis of fluorinated gold nanoclusters

Fluorinated gold nanoclusters were obtained by a modified Brust reaction, as previously reported by Dass and coworkers.[S5] Briefly, in a round-bottomed flask, tetraoctylammonium bromide (82 mg, 0.15 mmol, 1 eq) was dissolved in α,α,α-trifluorotoluene (30 mL). $HAuCl_4 \cdot 3H_2O$ (60 mg, 0.15 mmol, 1 eq) was separately dissolved in the minimum amount of Milli-Q water and added under vigorous stirring to the organic solution, which turned orange upon addition. The selected thiol was then added in the appropriate amount (details reported in Table S2) - either directly (PFDT) or dissolved in 1 mL of α,α,α-trifluorotoluene (**1**) - and the reaction mixture was stirred for additional 10 minutes, until colorless, and then cooled to 0 °C with an ice bath. An ice-cold solution of $NaBH_4$ (57 mg, 1.5 mmol, 10 eq) in Milli-Q water (4 mL) was added dropwise and the resulting mixture was vigorously stirred at 0 °C for 3 hours. The obtained dark brown organic phase was washed with Milli-Q water (3×25 mL) and evaporated at reduced pressure, at room temperature. The residue was then taken up with the minimum amount of toluene and transferred into a Falcon tube for purification. Purification was performed by repeating the following steps:

- ultrasound treatment (59 kHz) for 10 minutes
- centrifugation for 10 minutes (8694 rcf for **1**; 1717 rcf for PFDT)
- removal of the supernatant
- addition of clean toluene

After the last purification cycle, the supernatant was analyzed by ^{19}F and ^{1}H NMR (20% v/v $CDCl_3$ added for lock) to check the absence of excess of reagents. The remaining pellet was dried and dissolved in the minimum amount of Solkane®. The resulting dark solution was sonicated for 10 minutes, filtered through a 0.2 μm PTFE filter and stored at r.t. in screw-capped glass vials.

Table S2. Summary of all the NCs batches obtained with both PFDT and thiol **1**, indicating for each: mean diameter estimated from TEM statistical analysis (Ø), Au concentration (from ICP), and number of NCs per mL of stock solution.

Sample	Thiol	Molar ratio (thiol / $HAuCl_4$)	Ø (nm)	[Au] (mg/L)	[NCs] (NCs/mL)
PFDT-AuNCs	PFDT	3:1	2.3 ± 0.7	2000	$1.7*10^{16}$
SF-AuNCs1	**1**	3:1	1.4 ± 0.6	6032	$1.9*10^{17}$
SF-AuNCs2	**1**	6:1	1.1 ± 0.6	2072	$1.2*10^{17}$

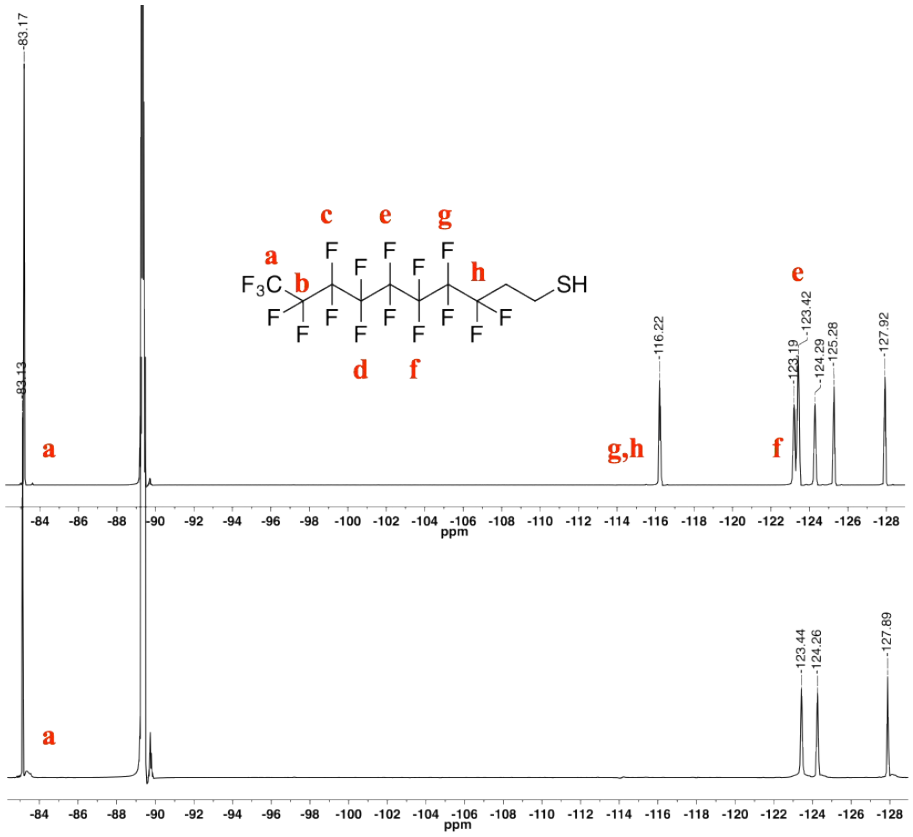

Figure S3. ^{19}F-NMR of PFDT (top) and **PFDT-AuNCs** (bottom) in Solkane (-89.5 ppm), with a C_6D_6 capillar for locking. The signals attributable to the fluorine atoms closest to the NC's core (e-h) disappear into the baseline due to the molecules packing on the NC's surface.

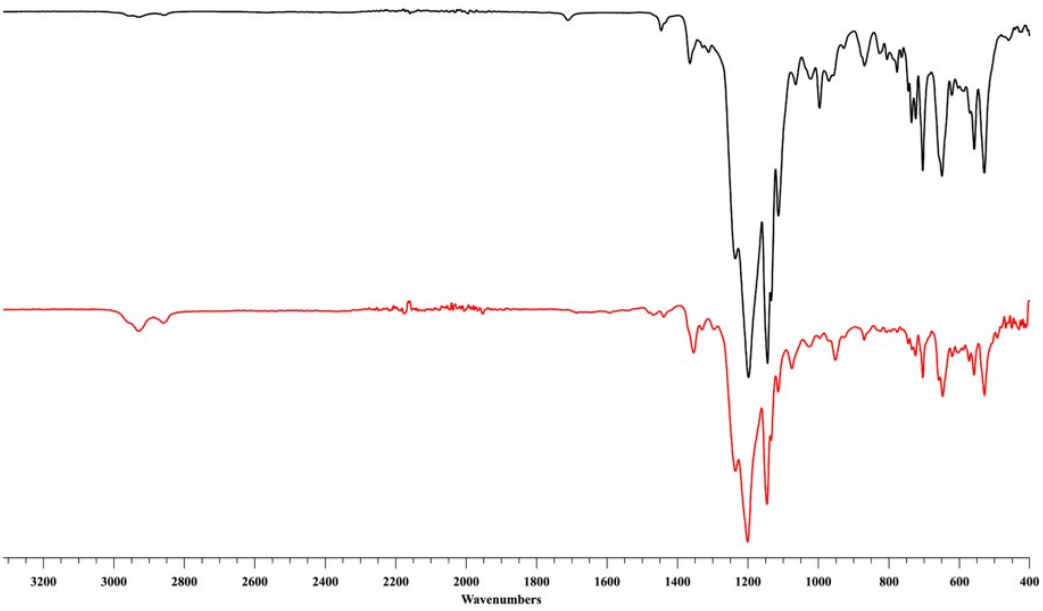

Figure S4. ATR FT-IR spectra of PFDT (black) and **PFDT-AuNCs** (red).

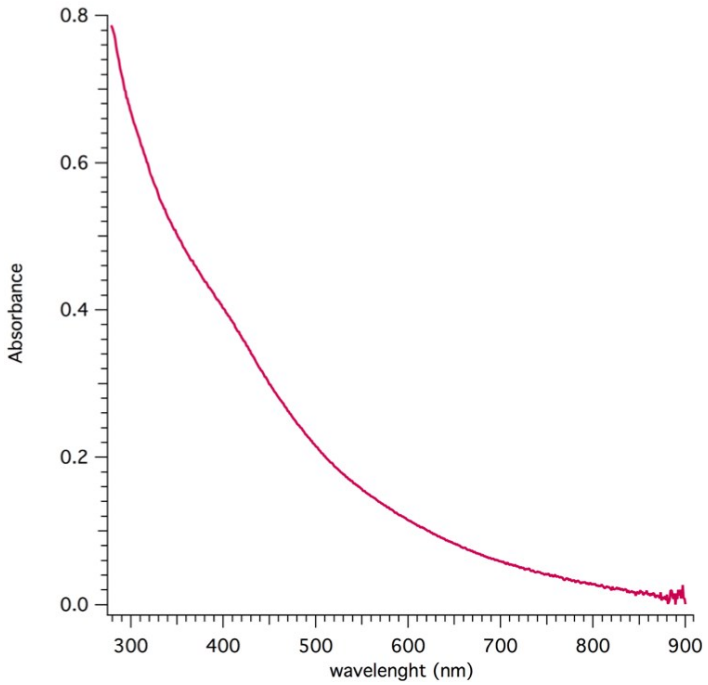

Figure S5. UV-vis absorption spectra of **PFDT-AuNCs** diluted solution in Solkane®.

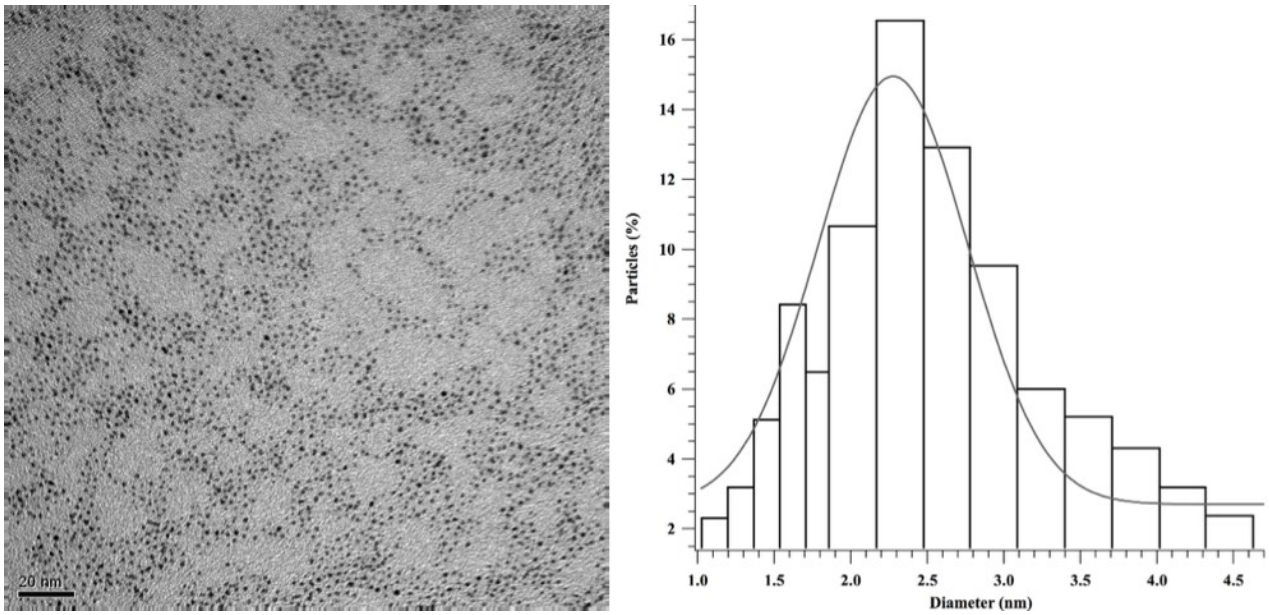

Figure S6. TEM image of **PFDT-AuNCs** (left) and corresponding statistical analysis of the particles diameters (right). The mean size is 2.3 ± 0.7 nm.

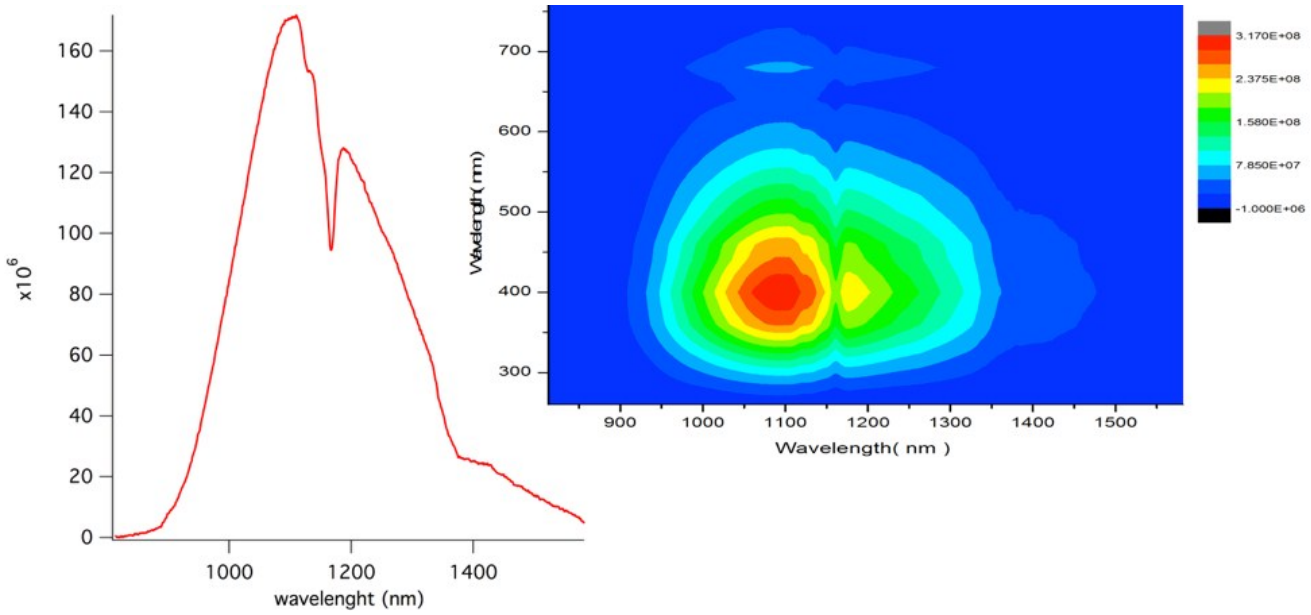

Figure S7. NIR-luminescence spectrum of **PFDT-AuNCs**, registered with excitation at 410 nm (left), and its NIR-luminescence 3D spectrum (right), showing emission wavelength (x axis), excitation wavelength (y axis) and intensity (z axis).

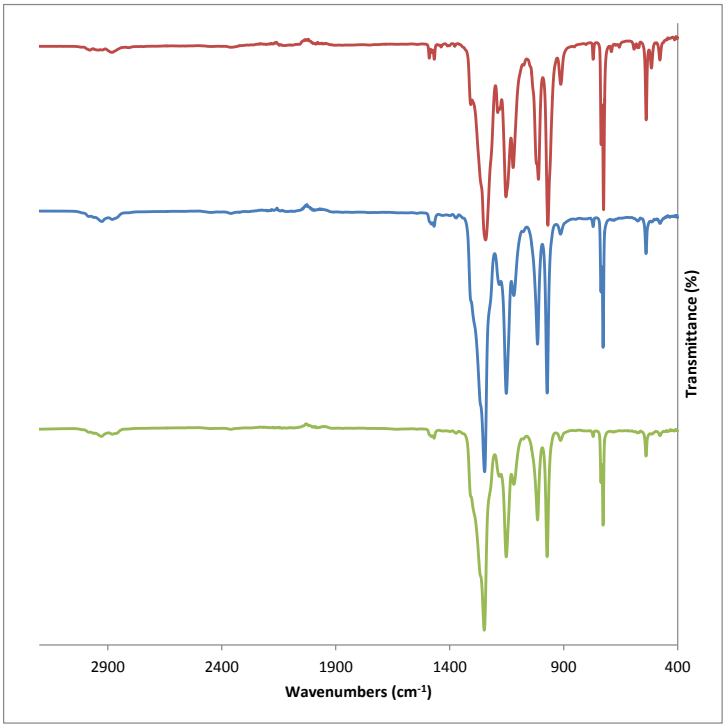

Figure S8. ATR FT-IR spectra of thiol **1** (red), **SF-AuNCs1** (blue) and **SF-AuNCs2** (green).

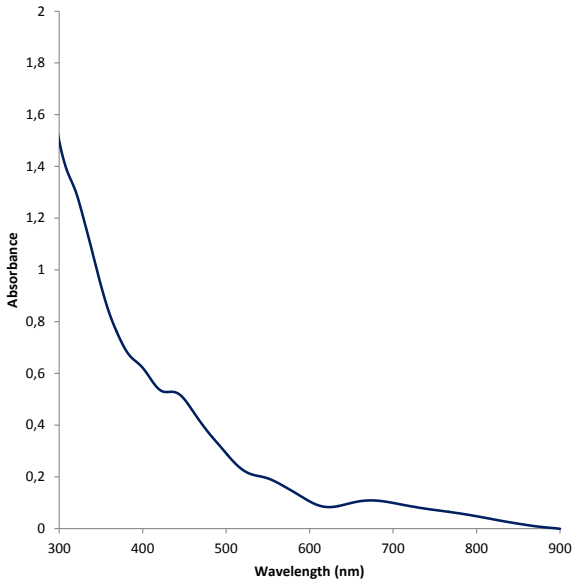

Figure S9. UV-vis absorption spectrum of **SF-AuNCs2** diluted dispersions in Solkane®.

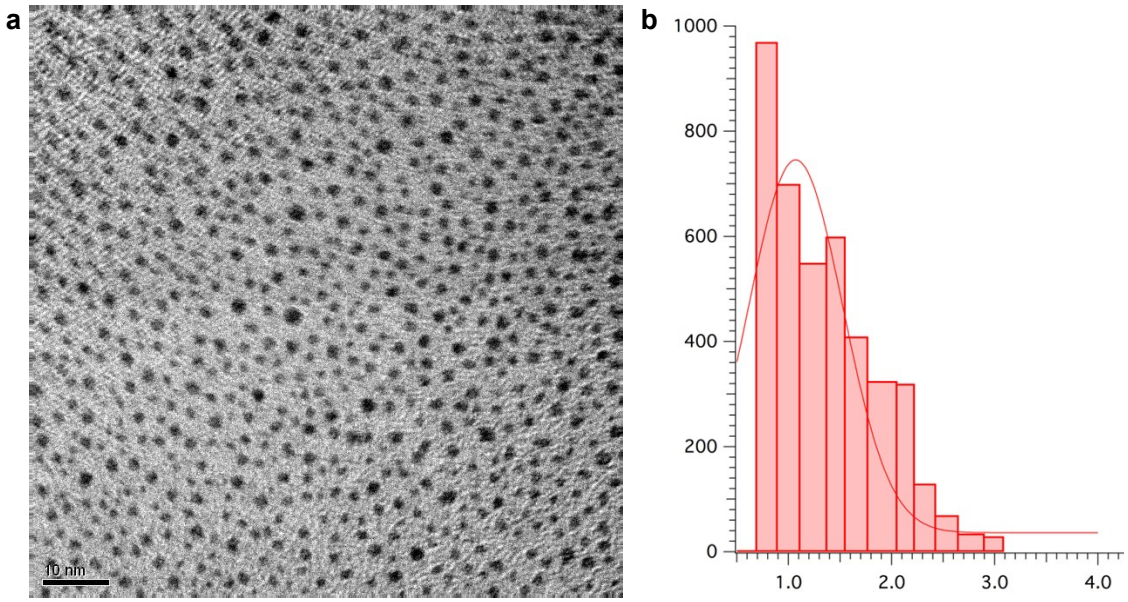

Figure S10. TEM image of **SF-AuNCs2** (a), and corresponding statistical analysis of NCs diameters (b). The mean size resulted to be 1.1 ± 0.6 nm.

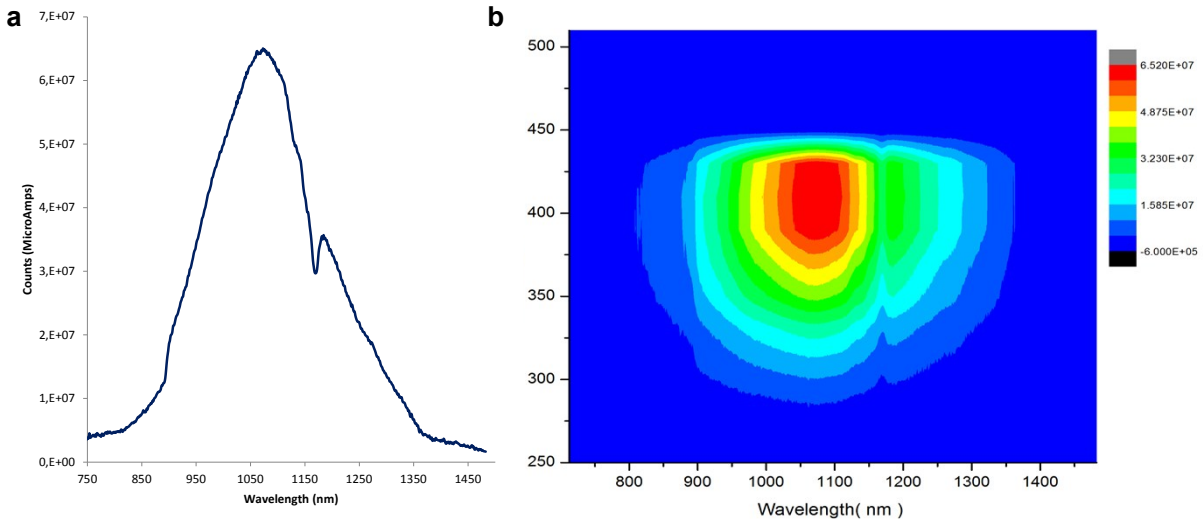

Figure S11. NIR-luminescence spectrum of **SF-AuNCs2**, registered with excitation at 410 nm (a), and its NIR-luminescence 3D spectrum (b), showing emission wavelength (x axis), excitation wavelength (y axis) and intensity (z axis).

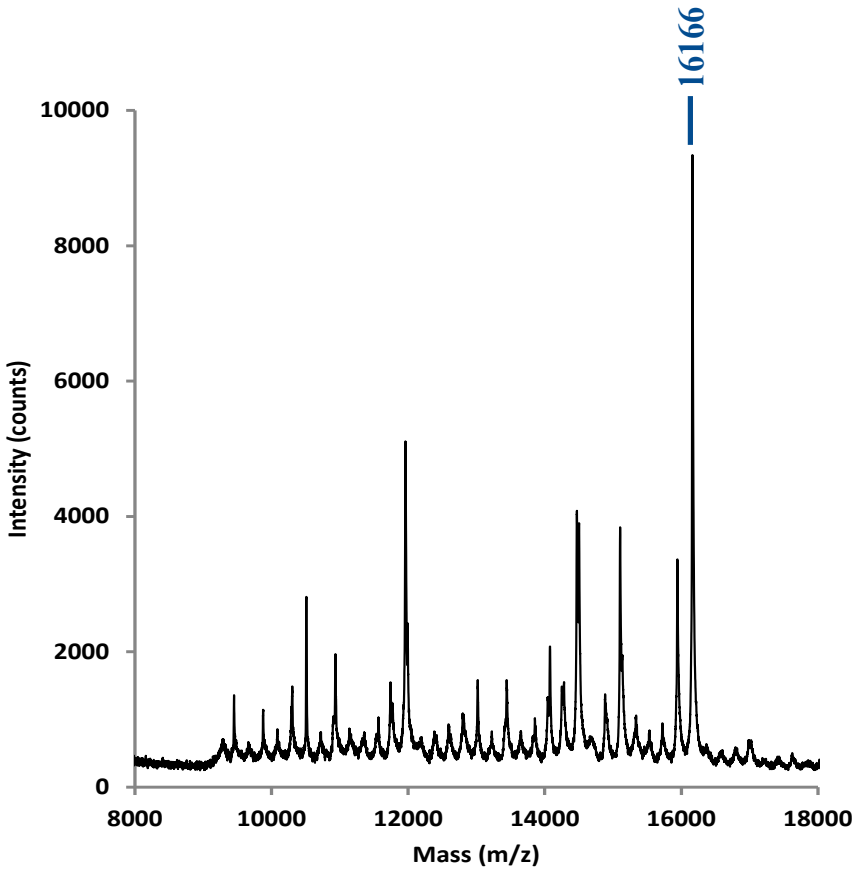

Figure S12. MALDI spectrum of a solkane dispersion of **SF-AuNCs1**, evidencing the predominant peak m/z value.

Table S3. ^{19}F (564.73 MHz) T_1 and T_2 relaxation values for thiol **1** and **SF-AuNCs1** measured at 293 K

Compound	Peaks (ppm)	Integral	T_1 (ms)	T_2 (ms)
Thiol 1	-71.15		960	500
SF-AuNCs1	-71.14	1	760	95
	-71.04	0.3	490	66
	-70.96	0.8	480	87

Preparation of SF-AuNCs1 loaded liposomes

Briefly, in a round-bottomed flask 50 μl of a solkane dispersion of **SF-AuNCs1** were added to a mixture of DOPC (10 mg) in chloroform (1 ml). The resulting mixture was evaporated under reduced pressure at r.t. until complete drying and then kept at 5 mbar for additional two hours. The obtained lipid film was then re-dispersed in MilliQ water (1 ml). The aqueous solution was subject of 5 cycles of freeze-thaw and passed through an extruder using first 200 nm and then 100 nm pores size filters. The final dispersion was analyzed via multiangle DLS, ^{19}F-NMR and fluorescence spectroscopy. DLS results of the pure liposomal dispersions and those containing **SF-AuNCs1** were very similar, thus the presence of **SF-AuNCs1** did not change the overall structure of the liposomes. Auto-correlation functions were analyzed with CONTIN and showed a monomodal size distribution with an averaged $<R_h>$ of about 60-70 nm. For some angles for some batches of both formulations it appeared a smaller population with an $<R_h>$ of about 15 nm.

Table S4. DLS results for a DOPC liposomal dispersions of **SF-AuNCs1** at different angles.

Angle (°)	**<Decay time (s)>**	**<Γ (s^{-1})>[a]**	**q^2 (nm^{-2})[b]**
50	0.0025	406.2	0.000124
70	0.0014	732.1	0.000229
90	0.0008	1169.3	0.000348
110	0.0006	1589.0	0.000468
130	0.0005	1978.6	0.000572

[a] Γ values were extrapolated from a CONTIN fit of the auto-correlation functions.

[b] $q^2=((4*\pi*n)/\lambda)*(\sin(\theta/2))$ where n=refractive index, λ=laser wavelength

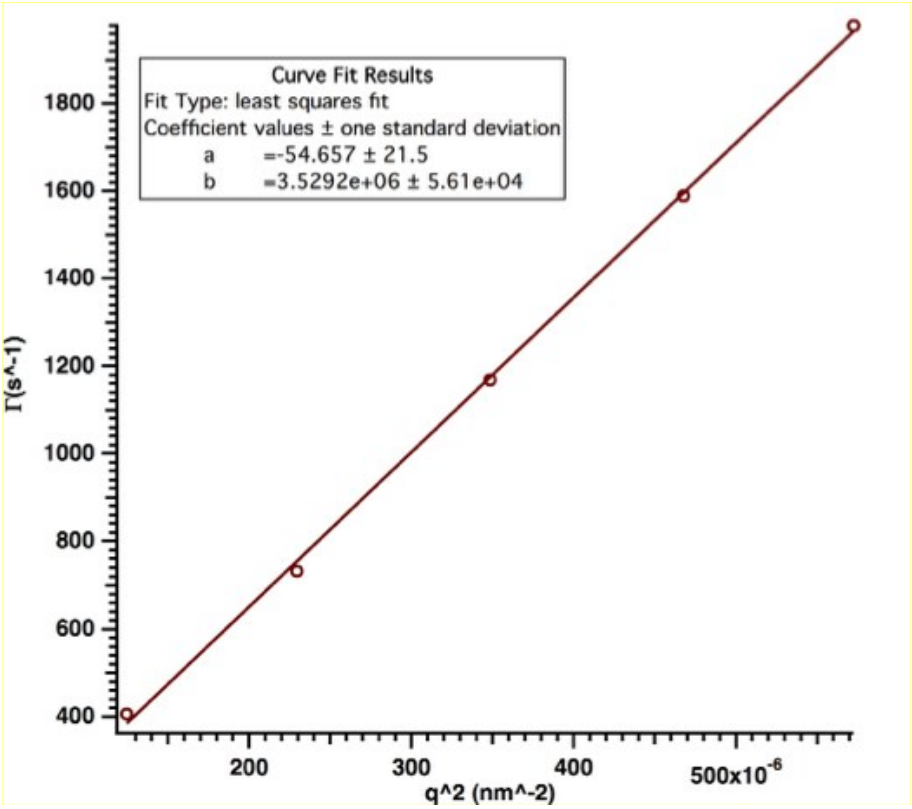

Fig. S13 Γ vs q^2 graph of a DOPC liposomal dispersion of **SF-AuNCs1**. (R_h= 69.5 nm)

Table S5. DLS data for a DOPC liposomal dispersion at different angles.

Angle (°)	Decay time (s)	Γ (s^{-1})[a]	q^2 (nm^{-2})[b]
50	0.0025	405.0	0.000124
70	0.0013	744.6	0.000229
90	0.00087	1151.0	0.000348
110	0.0006	1590.1	0.000468
130	0.0005	1965.0	0.000572

[a] Γ values were extrapolated from a CONTIN fit of the auto-correlation functions.

[b] $q^2=((4*\pi*n)/\lambda)*(\sin(\theta/2))$ where n=refractive index, λ=laser wavelength

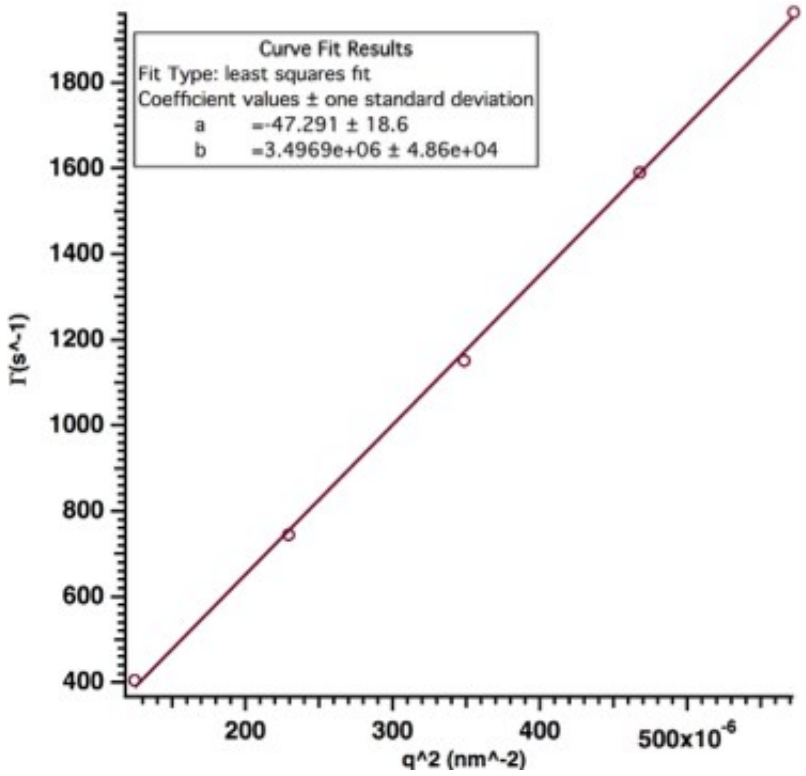

Fig. S14 Γ vs q^2 graph of a DOPC liposomal dispersion, obtained from a mixture of chloroform and Solkane. (R_h= 70.2 nm)

Molecular Mechanics (MM) and Molecular Dynamics (MD)

The influence of the curvature of an ideal gold nanosphere and the interaction among fluorinated chains attached on the gold nanosphere was theoretically studied using *InsightII/Discover 2000* package, distributed by Accelrys Inc.[S6] (San Diego, CA) using the consistent valence force field CVFF with a Morse potential for the bonded atoms.[S7] All the energy minimizations were carried out up to an energy gradient lower than 4×10^{-3} kJ mol^{-1} Å^{-1} *in vacuo* without any constraint on the atoms freedom of motion, including also the gold atoms of the nanosphere. The MD runs were performed at a room constant temperature (T = 300 K) controlled through the Berendsen thermostat. Integration of the dynamical equations was carried out with the Verlet algorithm using a time step of 1 fs, and the instantaneous coordinates were periodically saved for further analysis or geometry optimization.[S8-S9] The length of the MD run was 5 ns for the gold nanosphere isolated having a diameter equal to 12 Å in order to study the influence of the curvature of the substrate, and 25 ns when four, five, six, seven and eight fluorinated chain were attached to the nanosphere through covalent bonds of the sulphur atom with surface gold atoms, as shown in Fig. 4a. Finally, the MD run of the functionalized nanosphere comprising 82 gold atoms as the experimental one lasted for 100 ns. In particular, within this MD runs, the time changes of the total and potential energy together with its components were monitored. These quantities showed a decrease within the initial 30 ns, and then fluctuated around a constant value, indicating achievement of equilibrium, as reported for example in the Fig. S15.

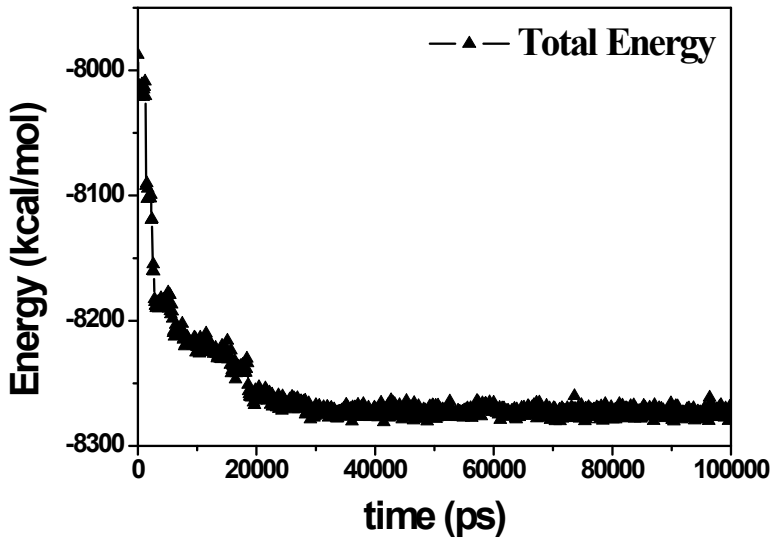

Fig. S15 Total energy as a function of the MD run time simulation of the ideal gold nanosphere having eight fluorinated chain.

The Radial Distribution Function RDF, reported in Fig. 4b, calculated within an MD trajectory, gives the probability density of finding a chosen set of all the fluorine atoms, indicated in light blue in Fig. S16, as a function their distance *r* from the centre of mass of the gold nanosphere indicated in yellow.

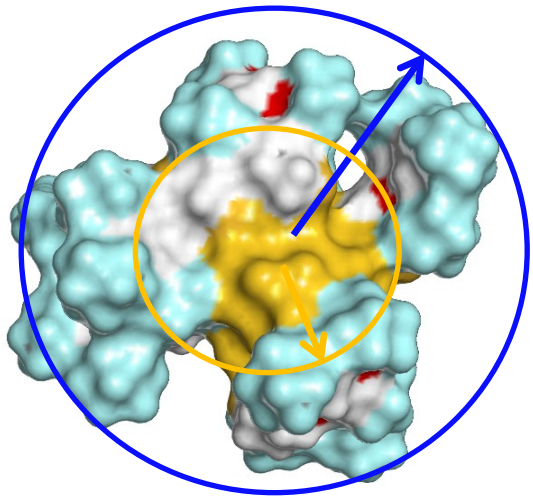

Fig. S16 Optimized geometry after MD run at room temperature of simulated nanosphere using MM and MD methods.

References

[S1] X. Yue, M. B. Taraban, L. L. Hyland and Y. B. Yu, *J. Org. Chem.*, 2012, **77**, 8879-8887.

[S2] G. M. Sheldrick, *Acta Crystallogr. Sect. A*., 2008, **64**, 112-122.

[S3] C. F. Macrae, I. J. Bruno, J. A. Chisholm, P. R. Edgington, P. McCabe, E. Pidcock, L. Rodriguez-Monge, R. Taylor, J. van de Streek and P. A. Wood, *J. Appl. Cryst*., 2008, **41**, 466-470.

[S4] E. F. Pettersen, T. D. Goddard, C. C. Huang, G. S. Couch, D. M. Greenblatt, E. C. Meng and T. E. Ferrin, *J. Comput. Chem.*, 2004, **25**, 1605-1612.

[S5] A. Dass, R. Guo, J. B. Tracy, R. Balasubramanian, A. D. Douglas and R. W. Murray, *Langmuir*, 2008, **24**, 310-315.

[S6] Accelrys Inc. *InsightII 2000*; Accelrys Inc.: San Diego, CA, 2000. See also http://www.accelrys.com.

[S7] P. Dauber-Osguthorpe, V. A. Roberts, D. J. Osguthorpe, J. Wolff, M. Genest and A. T. Hagler, *Proteins: Struct. Funct. Genet.*, 1988, **4**, 31-47.

[S8] G. Raffaini and F. Ganazzoli, *J. Chromatography* A, 2015, **1425**, 221-230.

[S9] G. Raffaini, F. Ganazzoli and A. Mazzaglia, *Beilstein J. Org. Chem.*, 2016, **12**, 73-80.